

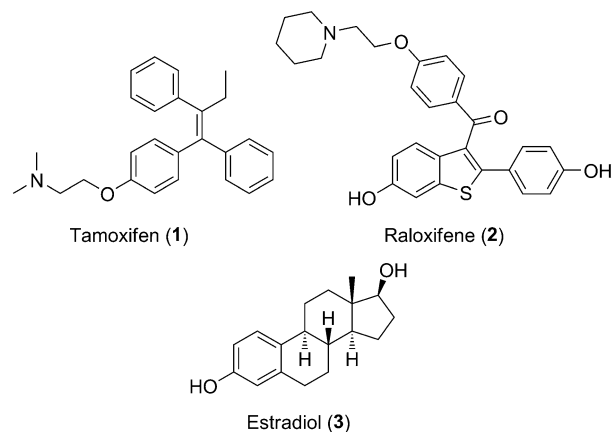
DOI: 10.1002/cmdc.201200307

Discovery of a New Class of Liver Receptor Homolog-1 (LRH-1) Antagonists: Virtual Screening, Synthesis and Biological Evaluation

Jullien Rey,^[a] Haipeng Hu,^[b] Fiona Kyle,^[c] Chun-Fui Lai,^[c] Laki Buluwela,^[c] R. Charles Coombes,^[c] Eric A. Ortlund,^[d] Simak Ali,^{*,[c]} James P. Snyder,^{*,[b]} and Anthony G. M. Barrett^{*,[a]}

After lung cancer, breast cancer in women is the most common cancer in the world with more than a million new cases diagnosed every year.^[1] Estrogens, acting through the estrogen receptor, are important drivers of breast cancer growth. Much progress has been made in the fight against breast cancer with the development of antiestrogen agents, such as tamoxifen (1) and raloxifene (2), capable of competing with the agonistic action of estradiol (3) at the estrogen receptor α (ER α).^[2] Estrogen binding to the ligand binding domain (LBD) of ER α generates a receptor conformation that reveals a co-activator recruitment groove involving α -helices 3, 4, 5 and 12, allowing co-activator recruitment to agonist-bound ER and consequent stimulation of gene expression. Through helix 12 (H12) displacement, antiestrogen agents can prevent the formation of the ER α LBD co-activator binding surface, thereby preventing co-activator recruitment and subsequent stimulation of gene expression.^[3] However, resistance to these therapies is common, and so the identification of new molecular targets for breast cancer treatment is an important goal.

Liver receptor homolog-1 (LRH-1) is a member of the steroidogenic factor subfamily of nuclear receptors (NR) and plays a prominent role in both adult and developmental biology.^[4] It has also been implicated in the control of aromatase expression in breast tumor-associated stroma, stimulating local estrogen biosynthesis.^[5] Recently, LRH-1 was identified as a key regulator of ER expression in breast cancer cells^[6] and was shown to be associated with invasive breast cancer and estrogen-dependent cell proliferation.^[7] Together, these findings suggest that the development of a small molecule capable of antagonizing LRH-1 could provide a powerful new strategy for inhibiting estrogen signaling for the treatment of breast cancer.



Co-activator recruitment to the LBD of NRs is mediated by α -helical motifs in co-activator proteins conforming to the consensus sequence LXXXLL, where L is leucine and X is any amino acid.^[8,9] As is the case for ER α , agonist binding to other NRs reveals a co-activator recruitment groove that can accommodate the α -helical LXXXLL region.^[10] This well-studied molecular switch, with conformational changes in the LBD allowing co-activator recruitment and antagonist binding blocking co-activator recruitment, provides a powerful screening strategy for identifying NR agonists and antagonists. Using a high-throughput screening (HTS) strategy based on interaction between the LRH-1 LBD and a LXXXLL motif in the NR co-activator, transcriptional intermediary factor 2 (TIF2) in a fluorescence resonance energy transfer (FRET)-based assay, Whitby et al. discovered a series of substituted *cis*-bicyclo[3.3.0]oct-2-enes acting as LRH-1 agonists.^[11] However, to the best of our knowledge, no antagonist has yet been reported in the literature, making the development of such molecules an attractive and challenging task.

While LRH-1 is known to bind phospholipids, recent structural studies of LRH-1 suggest that these phospholipids are exchangeable with exogenous compounds and that a pool of apoLRH-1 exists in cells.^[12,13] Given the availability of large chemical libraries, we employed virtual HTS and molecular modeling strategy to identify potential LRH-1 antagonists. Such compounds were assumed to bind within the LRH-1 LBD, displacing the mobile α -helix H12 by means of α -helix–small molecule steric clashes, and thereby, generate an inactive conformation. Using raloxifene (2) as a search template, a two-dimensional virtual HTS of the ChemNavigator library,^[14] which contains 50 million-plus compounds, delivered 974 hits. Subsequent docking-based three-dimensional screening of the latter dataset with the Glide/molecular mechanics generalized Born

[a] Dr. J. Rey, Prof. A. G. M. Barrett
Department of Chemistry, Imperial College London
London, SW7 2AZ (England)
E-mail: agm.barrett@imperial.ac.uk

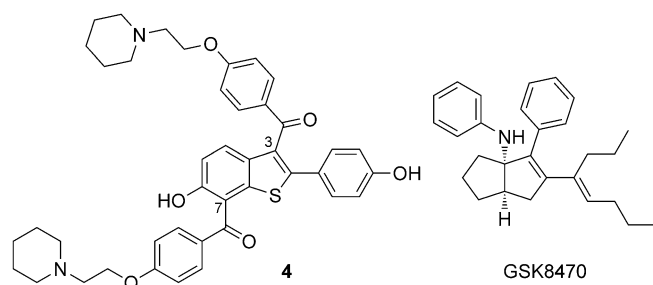
[b] Dr. H. Hu, Prof. J. P. Snyder
Department of Chemistry and Emory Institute for Drug Development
Emory University
1515 Dickey Drive, Atlanta, GA 30322 (USA)
E-mail: jsnyder@emory.edu

[c] Dr. F. Kyle, C.-F. Lai, Dr. L. Buluwela, Prof. R. C. Coombes, Prof. S. Ali
Department of Surgery and Cancer, Imperial College London
London, W12 0NN (England)
E-mail: simak.ali@imperial.ac.uk

[d] Prof. E. A. Ortlund
Department of Biochemistry, Emory University, School of Medicine
1510 Clifton Rd NE, Atlanta, GA 30322 (USA)

Supporting information for this article is available on the WWW under <http://dx.doi.org/10.1002/cmdc.201200307>.

surface area (MMGBSA) algorithms^[15,16] and the hLRH-1 LBD crystal structure housing phosphatidyl glycerol (PG) (PDB: 1YOK;^[17] PG removed for docking) led to identification of the benzothiophene analogue **4**. Given the flexibility of nuclear receptors,^[18,19] it would have been ideal to work with LRH-1 bound by an antagonist. However, in the absence of such a structure, 1YOK was selected since PG is a large, weak agonist whose binding pocket is expanded by comparison with a smaller potent agonist; the pocket created by PG can be considered as more suitable for antagonist binding (see Figure S1 in the Supporting Information).



Docked into LRH-1, structure **4** adopted the desired antagonistic pose in which the C-7 side chain promotes virtual H12 displacement (Figure 1 a). The benzothiophene core of **4** coincides with the binding pose of the GSK8470 agonist in the X-ray-determined complex (PDB: 3PLZ;^[11b] Figure 1 b). The antagonist is anchored in the pocket primarily by hydrophobic interactions between the core and the C-3 and C-7 side chains. The C-3 side chain is surrounded by H6 and H7, and the hairpin linking H5 and H6. The C-7 piperidine side chain, on the other

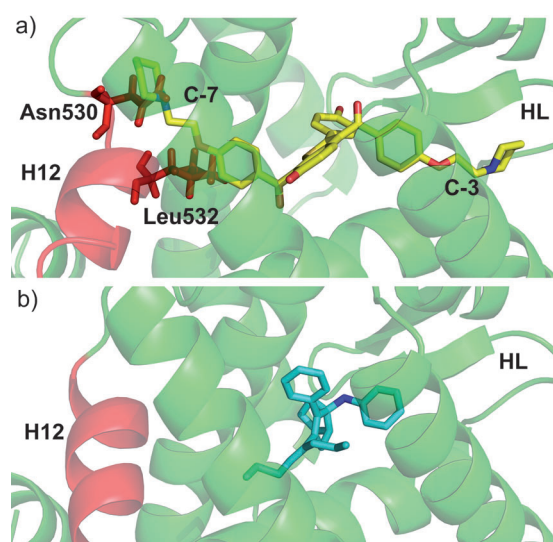


Figure 1. Small molecules in the ligand binding domain (LBD) of LRH-1. a) Molecular modeling (docking pose) of benzothiophene antagonist **4** in LRH-1. Helix 12 (H12) in the phosphatidyl glycerol-bound protein is highlighted in red (PDB: 1YOK^[17]). Also shown is the hairpin loop (HL) linking H5 and H6. The residues Asn 530 and Leu 532 of H12 are highlighted as red sticks. b) Whitby agonist GSK8470/LRH-1 X-ray structure (PDB: 3PLZ^[11b]).

hand, extends deeply into the space occupied by the side chains of residues Asn530 and Leu532 of H12, causing very serious steric clashes (Figure 2). This modeled juxtaposition was precisely that sought to displace H12.

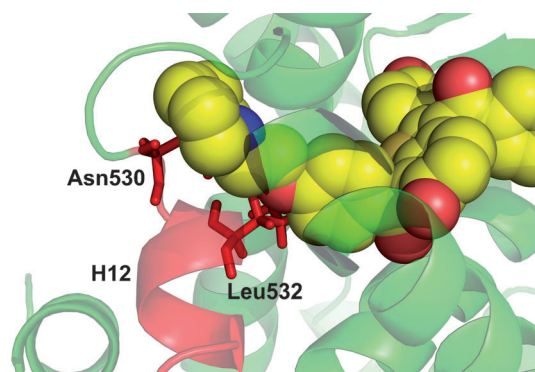
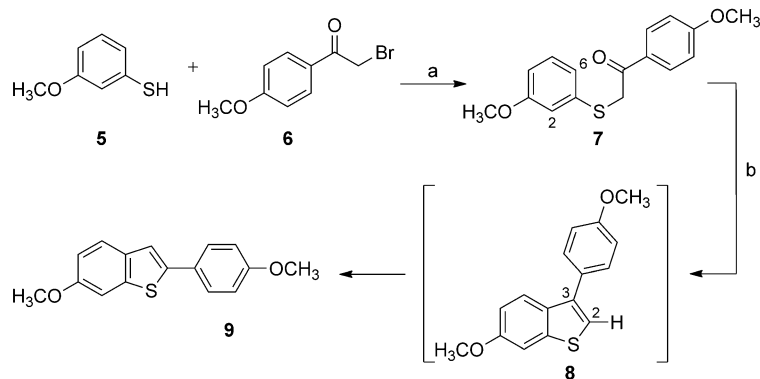


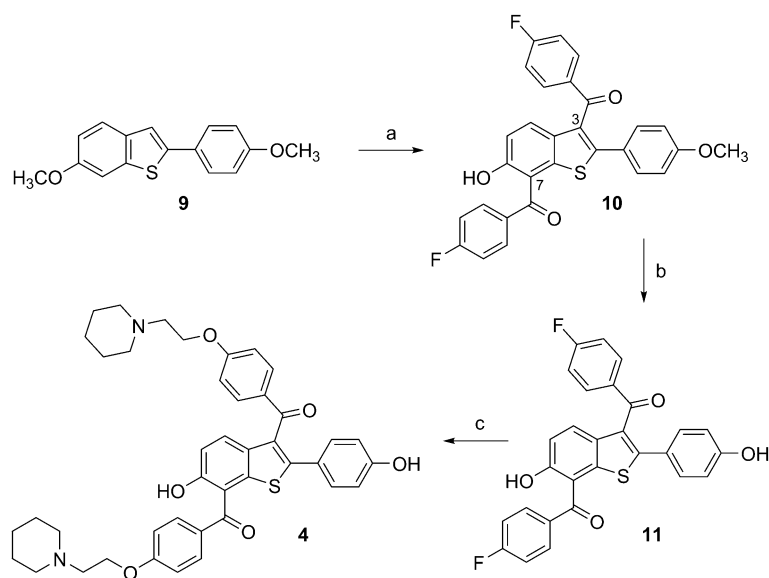
Figure 2. Interpenetration of the ethoxypiperidine moiety of **4** (space-filled structure) into helix 12 (H12). Structure **4** is docked into LRH-1 (PDB: 1YOK^[17]) without H12 and overlaid with the same receptor retaining H12 in place (red). Leu532 (red sticks) pierces the C-7 CH₂O-phenyl segment of **4**, while Asn530 passes through the center of the distal piperidine ring.

In order to validate the docking predictions, the synthesis and biological evaluation of benzothiophene **4** were pursued. With no precedence in the literature for the selective introduction of benzoyl moieties at the C-7 position of a benzothiophene ring, a novel and efficient synthetic approach needed to be developed. Benzothiophene **9** was obtained in two steps by nucleophilic substitution of bromoketone **6** with thiophenol **5** and subsequent cyclization in neat polyphosphoric acid at 90 °C (Scheme 1).^[20] Under these conditions, a mixture of isomers was formed as the cyclization can occur either at the *ortho*- or *para*-position of the methoxy group (positions 2 and 6 from **7**). Pleasingly, the compounds could be separated by selective crystallization from refluxing acetone, giving the less soluble and major benzothiophene isomer **9**. Mechanistically, the formation of benzothiophene **9** goes via the formation of C-3-substituted intermediate **8** through acid-catalyzed hydroalkylation by the protonated ketone **7** followed by aromatization. Protonation of intermediate **8** followed by a 3,2-shift of the methoxyphenol ring and aromatization led to desired product **9**.^[21]

A double Friedel–Crafts acylation was examined in an attempt to functionalize both the C-3 and C-7 positions of the benzothiophene ring (Scheme 2). Aluminum-chloride-mediated double acylation using an excess of 4-fluorobenzoyl chloride was accompanied by partial selective demethylation and gave benzophenone **10**. Selective mono-deprotection of related aryl methyl ethers is known to proceed via the formation of a six-membered ring chelate between the aluminum, the *ortho*-ketone carbonyl, and the phenolic oxygen atom leading to, in this case, phenol **10**.^[22] This was further demethylated using boron tribromide to produce diphenol **11**. Finally, the piperidine side chains were introduced by nucleophilic aromatic substitutions generating benzothiophene **4**.^[23]



Scheme 1. Synthesis of benzothiophene intermediate **9**. Reagents and conditions: a) KOH, EtOH, H₂O, RT, 18 h, 81%; b) polyphosphoric acid, 90 °C, 1 h, 63%.



Scheme 2. Synthesis of benzothiophene **4**. Reagents and conditions: a) 4-fluorobenzoyl chloride, AlCl₃, CH₂Cl₂, RT, 18 h, 70%; b) BBr₃, CH₂Cl₂, 0 °C, 3 h, 79%; c) 1-(2-hydroxyethyl)piperidine, NaH, DMF, 50 °C, 5 h, 52%.

To assay for inhibition of co-activator binding, benzothiophene **4** was tested in an in vitro assay using the bead-based proximity AlphaScreen method that allows sensitive measurement of protein–protein interactions by transfer of energy from the excited donor bead to an acceptor bead in close proximity,^[24] allowing screening for compounds that promote or inhibit protein–protein interactions. To determine inhibition of LRH-1/co-activator interaction, an assay was developed to measure co-activator recruitment by the LBD of LRH-1, using a biotinylated peptide derived from human PGC1 α , with the sequence 138-AEEPSSLKLLLLAPANT, and his-tagged, purified recombinant human LRH-1 LBD (amino acids 291–541).

Streptavidin-coated donor beads were incubated with the biotinylated co-activator peptide, together with his-tagged LRH-1 and nickel-nitrilotriacetic acid (Ni-NTA) acceptor beads. Since recombinant LRH-1 LBD takes up the activated conformation due to bound phospholipids,^[17,25] potential antagonists can readily be identified by a decrease in interaction with the

PGC1 α peptide. Gratifyingly, compound **4** exhibits LRH-1 antagonism in the low micromolar range (IC₅₀ = 3.1 μ M; Table 1), which is ideal for potency improvement by molecular manipulation. For example, the LRH-1 agonist GSK8470 has reported EC₅₀ values of 0.43–0.63 μ M, while chemical modification of the structure achieved derivatives with potencies as low as 10–100 nM.^[11]

An initial attempt to optimize **4** was motivated by a desire to decrease the molecular weight (**4**, MW = 704.9 amu) and improve the analogue physical properties within the context of the present synthetic scheme. The concept eliminates the C-7 ethoxypiperidine in **4**, but compensates its predicted steric effect by replacing the C-7 aryl *meta*-hydrogen atoms with

methyl groups. Figure 2 illustrates an apparent severe steric encounter between the H12 Leu532 residue and the *meta*-centers of the aromatic ring. Docking structures **19** and **20** carrying one and two *meta*-methyl groups, respectively, into the LRH-1 LBD pocket (H12 removed) revealed predicted binding poses similar to **4**. A prospective clash of the alkylated aromatic rings with Leu532, consistent with antagonism, is evident (see Figure S2 in the Supporting Information). Accordingly, methylated analogues **19** and **20** (MW = 591.7 and 605.7 amu, respectively) were chosen for synthesis and bioassay.

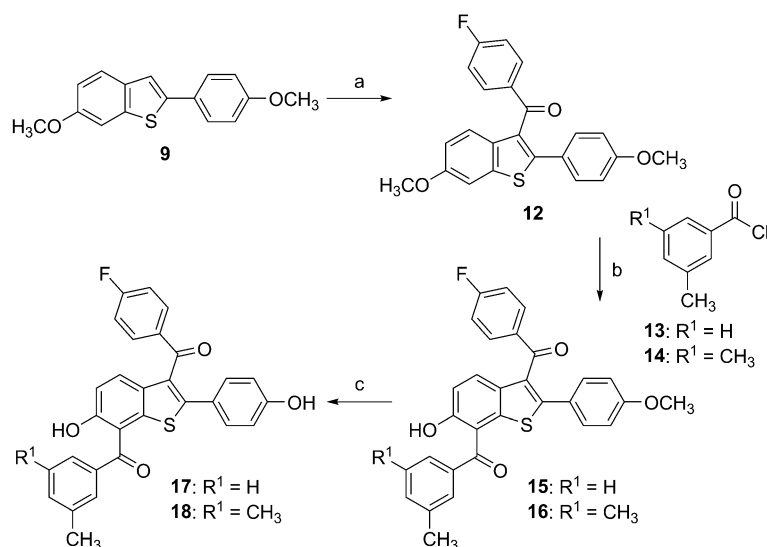
Both substituents at C-3 and C-7 positions were introduced

Table 1. Biological and computational evaluation of benzothiophene analogues conceived by virtual database screening and molecular modeling.

Entry	Compd	IC ₅₀ ^[a] [μ M]	Δ G [Kcal mol ⁻¹]
1	4	3.1 (2.6–3.7)	–136.7
2	19	5.8 (4.3–7.7)	–132.2
3	20	8.8 (5.1–15.0)	–130.9

[a] Data are the mean values of three experiments. The corresponding 95% confidence range is given in parentheses. [b] The MMGBSA algorithm was used to predict the binding affinities of these compounds for LRH-1.

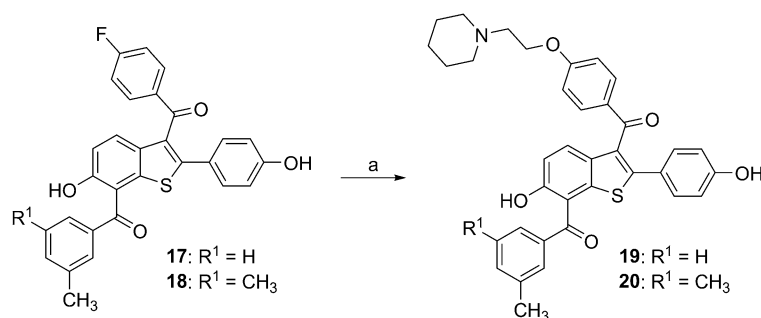
by sequential Friedel–Crafts acylation reactions. Reaction of benzothiophene **9** with one equivalent of 4-fluorobenzoyl chloride and aluminum chloride gave ketone **12** in a selective manner without formation of bis-acylated intermediate **10**



Scheme 3. Synthesis of benzothiophenes **17** and **18** by sequential Friedel–Crafts acylations. *Reagents and conditions:* a) 4-fluorobenzoyl chloride, AlCl₃, CH₂Cl₂, 18 h, 69%; b) AlCl₃, CH₂Cl₂, RT, 18 h; c) BBr₃, CH₂Cl₂, 0 °C, 3 h, for **17**: 42%, for **18**: 46% (two steps).

(Scheme 3)^[23] Subsequent acylation of benzothiophene **12** with 3-methylbenzoyl chloride (**13**) gave **15**, which was directly demethylated using boron tribromide to yield phenol **17**. Finally, nucleophilic aromatic substitution of fluoride **17** by 1-(2-hydroxyethyl)piperidine gave the desired benzothiophene **19** in moderate yield (Scheme 4). A similar strategy was used for the synthesis of benzothiophene **20** starting from intermediate **12** and 3,5-dimethylbenzoyl chloride (**14**) (Schemes 3 and 4).

Benzothiophenes **19** and **20** were then tested in the in vitro AlphaScreen assay to show a two to threefold decrease in antagonistic activity relative to **4** (Table 1). This result was examined by evaluating the MMGBSA free energies of binding^[16] for the three compounds. The order of binding is estimated to be **4** > **19** > **20** precisely in parallel with the in vitro results (Table 1). Consistently, the geometries of the docked structures suggest productive ligand contacts, and the degree of perturbation of Leu 532 on H12 by the ligands falls in the same order (see Figure S2 in the Supporting Information). It would appear that to achieve more effective antagonists, the longer C-7 side chain will need to be retained so as to penetrate well into H12



Scheme 4. Synthesis of benzothiophenes **19** and **20**. *Reagents and conditions:* a) 1-(2-hydroxyethyl)piperidine, NaH, DMF, 50 °C, 5 h, for **19**: 37%, for **20**: 35%.

space, while simultaneously maintaining suitable drug-like physical properties.

A mammalian two-hybrid assay was used to confirm the in vitro findings. For this, COS-1 cells were co-transfected with GAL4(DBD)-PGC1 α DNA binding domain and VP16-LRH-1, together with a GAL4-responsive luciferase reporter gene. As expected, GSK8470 stimulated the interaction of LRH-1 with PGC1 α (Figure 3). Raloxifene (**2**) weakly inhibited the interaction at concentrations up to 10 μ M. Inhibition by compounds **4**, **19** and **20** was again observed, with the degree of inhibition at 10 μ M being in the order **4** > **19** > **20**, as observed in the AlphaScreen assay. Investigation of the action

of these compounds towards ER α showed that they do indeed inhibit ER α in reporter gene assays, albeit considerably less potently than raloxifene (Figure S3 in the Supporting Information). GSK8470 had little or no effect on ER α activity.

In summary, three novel benzothiophene derivatives identified as modest LRH-1 antagonists using Glide/MMGBSA docking methodology were synthesized and biologically assayed. The identification of these analogues, derived by weak similarity comparisons to the selective estrogen receptor modulator (SERM) raloxifene (**2**), arose from high-throughput virtual screening performed on a library of millions of compounds. LRH-1 docking analysis suggests that the C-7 moiety of the benzothiophene scaffold is directed toward H12 and can cause a significant steric clash between the ligand terminal atoms and the H12 α -helix. Efforts to further chemically modify the C-7 side chain to develop novel benzothiophenes with improved potency are underway.

Experimental Section

Chemistry

All chemicals were used as received or purified using standard procedures. Solvents were dried by standard techniques and distilled under N₂ before use. All experiments were carried out in oven-dried glassware under an inert atmosphere of N₂ or Ar. Analytical thin layer chromatography (TLC) was performed using pre-coated aluminum- or glass-backed plates (Merck silica gel 60 F₂₅₄), and plates were visualized by ultraviolet light and/or treatment with

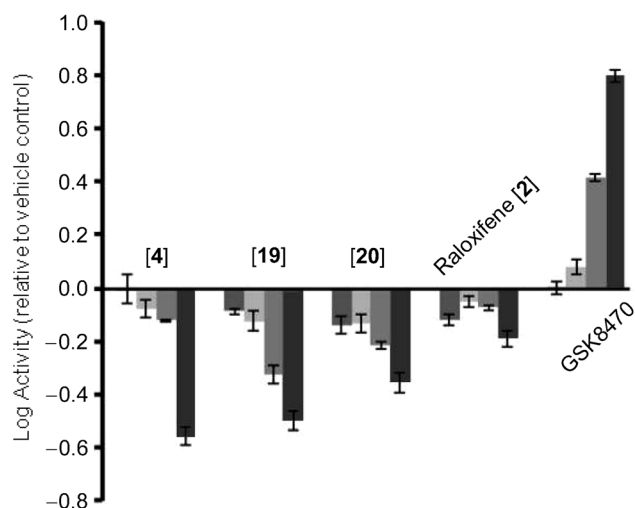


Figure 3. Mammalian two-hybrid analysis of compound activities in COS-1 cells: 0.01 μM : \blacksquare ; 0.1 μM : \square ; 1.0 μM : \blacksquare ; 10 μM : \blacksquare . COS-1 cells were transfected with GAL4(DBD)-PGC1 α L2 (encoding the second LXXLL motif in PGC1 α), VP16-LRH-1(LBD), together with a GAL4-responsive *Firefly* luciferase gene and pRL-CMV, which encodes *Renilla* luciferase and acts as a control for transfection efficiency. *Firefly* activities are shown relative to *Renilla* luciferase activities, the activity for vehicle (DMSO) being taken as 1 and all other activities calculated relative to this. The mean activities (Log 10) of three replicates are shown; error bars represent the standard error of the mean (SEM).

KMnO₄ or vanillin stains followed by heating as deemed appropriate. Flash column chromatography was carried out using silica (Merck 9385 Kieselgel 60; 230–400 mesh) under a positive pressure of N₂. ¹H and ¹³C NMR spectra were recorded at 400 or 500 MHz and 100 or 125 MHz, respectively. Chemical shifts (δ) are quoted in parts per million (ppm) and are referenced to a residual solvent peak. HSQC was used to confirm peak integration in ¹³C NMR spectra. Mass spectra were recorded using a Micromass Platform II and Micromass AutoSpec-Q spectrometer. The purity of the final compounds tested in vitro was assessed by LC/MS and HRMS. Infrared (IR) spectra were recorded using the attenuated total reflectance (ATR) technique, monitoring from 4000–700 cm⁻¹. Melting points (mp) were determined using a hot-stage microscope and are uncorrected.

Experimental protocols and characterization data for all intermediates are given in the Supporting Information.

2-(4-Hydroxyphenyl)-3,7-bis-((4-[2-(piperidin-1-yl)ethoxy]phenyl)carbonyl)-1-benzothiophen-6-ol (4): 1-(2-Hydroxyethyl)piperidine (66 μL , 0.49 mmol) was added with stirring to NaH (34 mg, 0.86 mmol, 60% in mineral oil) in DMF (1.4 mL) at RT. After 5 min, benzothiophene **11** (60 mg, 0.12 mmol) in DMF (0.20 mL) was added in one portion, and the mixture was stirred at 50 °C for 5 h. The reaction was quenched with H₂O, and the aqueous phase was extracted with EtOAc ($\times 3$). The combined organic extracts were washed with brine, dried (MgSO₄), filtered and concentrated in vacuo. Purification by flash chromatography (CH₂Cl₂/MeOH: 49:1 \rightarrow 24:1 + 0.25% NH₃·H₂O) gave diamine **4** as a yellow solid (45 mg, 52%): mp: 129–132 °C (MeOH); ¹H NMR (400 MHz, [D₆]DMSO): δ = 10.3 (br s, 1H), 9.74 (br s, 1H), 7.76 (d, J = 8.8 Hz, 2H), 7.68 (d, J = 8.8 Hz, 2H), 7.46 (d, J = 8.8 Hz, 1H), 7.15 (d, J = 8.8 Hz, 2H), 7.05 (d, J = 8.8 Hz, 2H), 6.92 (d, J = 8.8 Hz, 2H), 7.04 (d, J = 8.8 Hz, 1H), 6.65 (d, J = 8.8 Hz, 2H), 4.16 (t, J = 5.9 Hz, 2H), 4.08 (t, J = 5.9 Hz, 2H), 2.67 (t, J = 5.9 Hz, 2H), 2.61 (t, J = 5.9 Hz, 2H), 2.44–2.41 (m, 4H),

2.40–2.37 (m, 4H), 1.52–1.44 (m, 8H), 1.40–1.34 ppm (m, 4H); ¹³C NMR (100 MHz, [D₆]DMSO): δ = 193.3, 192.3, 162.8, 162.5, 157.8, 141.9, 138.4, 132.7, 131.8, 131.7, 129.9, 129.7, 129.5, 129.3, 125.8, 123.4, 118.4, 116.1, 115.6, 114.4, 114.2, 65.9 (2C), 57.1, 57.0, 54.3, 54.2, 25.5, 25.4, 23.8 (2C) ppm (one quaternary carbon obscured); IR (neat): $\tilde{\nu}$ = 1597, 1356, 1236, 1155, 900, 830 cm⁻¹; HRMS-ESI: m/z [M + H]⁺ calcd for C₄₂H₄₅N₂O₆S: 705.2998, found: 705.3010.

7-[(3-Methylphenyl)carbonyl]-2-(4-hydroxyphenyl)-3-((4-[2-(piperidin-1-yl)ethoxy]phenyl)carbonyl)-1-benzothiophen-6-ol (19): 1-(2-Hydroxyethyl)piperidine (33 μL , 0.25 mmol) was added with stirring to NaH (25 mg, 0.62 mmol, 60% in mineral oil) in DMF (1.4 mL) at RT. After 5 min, benzothiophene **17** (60 mg, 0.12 mmol) in DMF (0.20 mL) was added in one portion, and the mixture was stirred at 50 °C for 5 h. The reaction was quenched with H₂O, and the aqueous phase was extracted with EtOAc ($\times 3$). The combined organic extracts were washed with brine, dried (MgSO₄), filtered and concentrated in vacuo. Purification by flash chromatography (CH₂Cl₂/MeOH: 99:1 \rightarrow 19:1 + 0.25% NH₃·H₂O) gave amine **19** as an amorphous yellow solid (27 mg, 37%): ¹H NMR (400 MHz, [D₆]DMSO): δ = 10.4 (br s, 1H), 9.74 (br s, 1H), 7.68 (d, J = 9.3 Hz, 2H), 7.59 (s, 1H), 7.54 (d, J = 7.8 Hz, 1H), 7.51 (d, J = 8.8 Hz, 1H), 7.45 (d, J = 7.3 Hz, 1H), 7.40 (dd, J = 7.8, 7.3 Hz, 1H), 7.17 (d, J = 8.8 Hz, 2H), 7.05 (d, J = 8.8 Hz, 1H), 6.93 (d, J = 9.3 Hz, 2H), 6.66 (d, J = 8.8 Hz, 2H), 4.08 (t, J = 5.4 Hz, 2H), 2.62 (t, J = 5.4 Hz, 2H), 2.39–2.36 (m, 7H), 1.48–1.45 (m, 4H), 1.37–1.35 ppm (m, 2H); ¹³C NMR (125 MHz, [D₆]DMSO): δ = 195.2, 192.4, 162.8, 157.9, 155.0, 142.3, 138.8, 138.2, 137.7, 133.4, 132.9, 131.9, 129.8, 129.6, 129.3, 129.1, 128.3, 126.7, 126.3, 123.5, 117.9, 116.3, 115.7, 114.5, 65.9, 57.1, 54.3, 25.5, 23.8, 20.8 ppm; IR (neat): $\tilde{\nu}$ = 1653, 1594, 1503, 1429, 1387, 1287, 1248, 1164, 1030, 939, 841, 761 cm⁻¹; HRMS-ESI: m/z [M + H]⁺ calcd for C₃₆H₃₄NO₅S: 592.2158, found: 592.2156.

7-[(3,5-Dimethylphenyl)carbonyl]-2-(4-hydroxyphenyl)-3-((4-[2-(piperidin-1-yl)ethoxy]phenyl)carbonyl)-1-benzothiophen-6-ol (20): 1-(2-Hydroxyethyl)piperidine (32 μL , 0.24 mmol) was added with stirring to NaH (25 mg, 0.61 mmol, 60% in mineral oil) in DMF (1.4 mL) at RT. After 5 min, benzothiophene **18** (60 mg, 0.12 mmol) in DMF (0.20 mL) was added in one portion, and the mixture was stirred at 50 °C for 5 h. The reaction was quenched with H₂O, and the aqueous phase was extracted with EtOAc ($\times 3$). The combined organic extracts were washed with brine, dried (MgSO₄), filtered and concentrated in vacuo. Purification by flash chromatography (CH₂Cl₂/MeOH: 99:1 \rightarrow 19:1 + 0.25% NH₃·H₂O) gave amine **20** as an amorphous yellow solid (25 mg, 35%): ¹H NMR (400 MHz, [D₆]DMSO): δ = 10.4 (br s, 1H), 9.75 (br s, 1H), 7.68 (d, J = 8.8 Hz, 2H), 7.50 (d, J = 8.8 Hz, 1H), 7.37 (s, 2H), 7.27 (s, 1H), 7.17 (d, J = 8.3 Hz, 2H), 7.04 (d, J = 8.8 Hz, 1H), 6.92 (d, J = 8.8 Hz, 2H), 6.66 (d, J = 8.3 Hz, 2H), 4.08 (*app-br* t, 2H), 2.62 (*app-br* t, 2H), 2.39 (*app-br* s, 4H), 2.32 (s, 6H), 1.46 (*app-br* s, 4H), 1.36 ppm (*app-br* s, 2H); ¹³C NMR (125 MHz, [D₆]DMSO): δ = 195.4, 192.4, 162.8, 157.9, 154.8, 142.2, 138.7, 138.3, 137.5, 134.2, 132.8, 131.9, 129.8, 129.6, 129.3, 126.5 (3C), 123.5, 118.1, 116.3, 115.7, 114.5, 65.9, 57.1, 54.3, 25.5, 23.8, 20.7 ppm; IR (neat): $\tilde{\nu}$ = 1655, 1595, 1504, 1429, 1384, 1361, 1244, 1163, 1140, 1035, 939, 842, 763 cm⁻¹; HRMS-ESI: m/z [M + H]⁺ calcd for C₃₇H₃₆NO₅S: 606.2314, found: 606.2287.

Molecular modeling

For the preliminary virtual high-throughput screen, the ER α antagonist raloxifene was employed as a search template for mining of the ChemNavigator database. With compound similarity thresholds set at 55%, 974 structures were returned. The corresponding three-dimensional structures were generated by using LigPrep 2.3,

and conformational searches were performed with MacroModel 9.7.^[26] The ten conformers of each structure with the lowest calculated energy were selected as starting structures for docking. The LRH-1 LBD crystal structure (PDB: 1YOK^[17]) and the Glide docking procedure (Glide 5.5^[15]) in Maestro 9.0 were used to perform the docking studies.^[26] In order to mimic the inactive state of LRH-1, residues on H12 and the adjacent loop between H11 and H12 (residues 522–538) in the LRH-1 LBD were removed from the protein structure during the docking investigations. In the final step, a Prime 2.1^[26] MMGBSA rescoring^[16] was performed to predict the binding affinities of the test compounds for LRH-1.

Biology

AlphaScreen (amplified luminescent proximity homogenous assay) technology is a bead-based proximity assay consisting of a nickel-chelate-coated acceptor bead bound to a His-tagged LRH-1 LBD and a streptavidin-coated donor bead bound to a biotinylated co-activator peptide (PGC1 α). Following excitation with a high-intensity laser at 680 nm, a singlet ambient oxygen molecule forms on the surface of the donor bead with the ability to diffuse up to 200 nm. If an acceptor bead is within this proximity, the oxygen singlet reacts with a thioxene derivative on the acceptor bead, generating chemiluminescence and further activating a cascade of fluorophorescence emitting light at 520–620 nm, which can be used as a measurement of proximity/binding.

This system was optimized using LRH-1 with both PGC1 α and SRC2 (EC₅₀ = 35 nM and 369 nM, respectively, against 50 nM LRH-1) and robust assay “z” scores (z > 0.6). The system was validated using the known LRH-1 agonist GSK8470 with an EC₅₀ value of 220 nM.^[11a] The AlphaScreen system has been utilized previously to look at LRH-1 LBD co-factor recruitment.^[27] Using the interaction between a set concentration of LRH-1 and PGC1 α as a baseline, a twelve-point titration range of the experimental compounds was added to assess for inhibition of this interaction. The results were analyzed using Prism software, correcting for the background signal, and expressed as a percentage relative to a vehicle-treated control (DMSO). IC₅₀ values with 95% confidence intervals were then calculated. Further assay details have been included in the Supporting Information.

Acknowledgements

The authors are grateful to Cancer Research UK (CRUK) for financial support of this research. J.P.S. and H.H. thank Prof. Dennis Liotta (Emory University) for support of the modeling work. The authors also thank Prof. Donald McDonnell (Duke University) for his gift of VP16-LRH-1 and Gal4-PGC1 α constructs.

Keywords: antagonists • breast cancer • high-throughput virtual screening • ligand binding domains • nuclear receptor

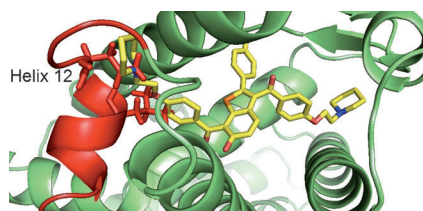
- [1] F. Kamangar, G. M. Dores, W. F. Anderson, *J. Clin. Oncol.* **2006**, *24*, 2137.
[2] S. Ali, L. Buluwela, C. R. Coombes, *Annu. Rev. Med.* **2011**, *62*, 217.

- [3] A. M. Brzozowski, A. C. W. Pike, Z. Dauter, R. E. Hubbard, T. Bonn, O. Engström, L. Öhman, G. L. Greene, J.-Å. Gustafsson, M. Carlquist, *Nature* **1997**, *389*, 753.
[4] E. Fayard, J. Auwerx, K. Schoonjans, *Trends Cell Biol.* **2004**, *14*, 250.
[5] C. D. Clyne, C. J. Speed, J. Zhou, E. R. Simpson, *J. Biol. Chem.* **2002**, *277*, 20591.
[6] P. T. R. Thiruchelvam, C.-F. Lai, H. Hua, R. S. Thomas, A. Hurtado, W. Hudson, A. R. Bayly, F. J. Kyle, M. Periyasamy, A. Photiou, A. C. Spivey, E. A. Ortlund, R. J. Whitby, J. S. Carroll, C. R. Coombes, L. Buluwela, S. Ali, *Breast Cancer Res. Treat.* **2011**, *127*, 385.
[7] A. L. Chand, K. A. Herridge, E. W. Thompson, C. D. Clyne, *Endocr.-Relat. Cancer* **2010**, *17*, 965.
[8] D. M. Heery, E. Kalkhoven, S. Hoare, M. G. Parker, *Nature* **1997**, *387*, 733.
[9] J. Torchia, D. W. Rose, J. Inostroza, Y. Kamei, S. Westin, C. K. Glass, M. G. Rosenfeld, *Nature* **1997**, *387*, 677.
[10] K. W. Nettles, G. L. Greene, *Annu. Rev. Physiol.* **2005**, *67*, 309.
[11] a) R. J. Whitby, S. Dixon, P. R. Maloney, P. Delerive, B. J. Goodwin, D. J. Parks, T. M. Willson, *J. Med. Chem.* **2006**, *49*, 6652; b) R. J. Whitby, J. Stec, R. D. Blind, S. Dixon, L. M. Leesnitzer, L. A. Orband-Miller, S. P. Williams, T. M. Willson, R. Xu, W. J. Zuercher, F. Cai, H. A. Ingraham, *J. Med. Chem.* **2011**, *54*, 2266.
[12] P. M. Musille, M. C. Pathak, J. L. Lauer, W. H. Hudson, P. R. Griffin, E. A. Ortlund, *Nat. Struct. Mol. Biol.* **2012**, *19*, 532.
[13] J. M. Lee, Y. K. Lee, J. L. Mamrosh, S. A. Busby, P. R. Griffin, M. C. Pathak, E. A. Ortlund, D. D. Moore, *Nature* **2011**, *474*, 506.
[14] ChemNavigator, 10919 Technology Place, Suite B, San Diego, CA 92127, USA; <http://www.chemnavigator.com/>.
[15] Glide (version 5.5), Schrödinger, LLC, 120 W. 45th Street, New York, NY 10036-4041, USA. For product details, see: <http://www.schrodinger.com/products/14/5/> (last accessed: August 22, 2012). For further reading, see: R. A. Friesner, J. L. Banks, R. B. Murphy, T. A. Halgren, J. J. Klicic, D. T. Mainz, M. P. Repasky, E. H. Knoll, D. E. Shaw, M. Shelley, J. K. Perry, L. C. Sander, P. S. Shenkin, *J. Med. Chem.* **2004**, *47*, 1739.
[16] A. P. Graves, D. M. Shivakumar, S. E. Boyce, M. P. Jacobson, D. A. Case, B. K. Shoichet, *J. Mol. Biol.* **2008**, *377*, 914.
[17] I. N. Krylova, E. P. Sablin, J. Moore, R. X. Xu, G. M. Waitt, J. A. MacKay, D. Juzumiene, J. M. Bynum, K. Madauss, V. Montana, L. Lebedeva, M. Suzawa, J. D. Williams, S. P. Williams, R. K. Guy, J. W. Thornton, R. J. Fletcher, T. M. Willson, H. A. Ingraham, *Cell* **2005**, *120*, 343.
[18] V. J. Hilser, E. E. Thompson, *J. Biol. Chem.* **2011**, *286*, 39675.
[19] M. Nocker, P. Cozzini, *Curr. Topics Med. Chem.* **2011**, *11*, 133.
[20] C. D. Jones, M. G. Jevnikar, A. J. Pike, M. K. Peters, L. J. Black, A. R. Thompson, J. F. Falcone, J. A. Clemens, *J. Med. Chem.* **1984**, *27*, 1057.
[21] H. Galons, J.-F. Girardeau, C. C. Farnoux, M. Miocque, *J. Heterocycl. Chem.* **1981**, *18*, 561.
[22] F. M. Dean, J. Goodchild, L. E. Houghton, J. A. Martin, R. B. Morton, B. Parton, A. W. Price, N. Somvichien, *Tetrahedron Lett.* **1966**, *7*, 4153.
[23] C. R. Schmid, J. P. Sluka, K. M. Duke, *Tetrahedron Lett.* **1999**, *40*, 675.
[24] J. Peppard, F. Glickman, Y. He, S.-I. Hu, J. Doughty, R. Goldberg, *J. Biomol. Screening* **2003**, *8*, 149.
[25] E. A. Ortlund, Y. Lee, I. H. Solomon, J. M. Hager, R. Safi, Y. Choi, Z. Guan, A. Tripathy, C. R. H. Raetz, D. P. McDonnell, D. D. Moore, M. R. Redinbo, *Nat. Struct. Mol. Biol.* **2005**, *12*, 357.
[26] MacroModel (version 9.7), LigPrep (version 2.3), Maestro (version 9.0), Prime (version 2.1), all from Schrödinger, LLC, 120 W. 45th Street, New York, NY 10036-4041, USA. For product details, see: <http://www.schrodinger.com/productsguide/>.
[27] Y. Li, M. Choi, K. Suino, A. Kovach, J. Daugherty, S. A. Kliewer, H. E. Xu, *Proc. Natl. Acad. Sci. USA* **2005**, *102*, 9505.

Received: June 20, 2012
Published online on ■■■■■, 0000

COMMUNICATIONS

Targeting LRH-1: Virtual screening and molecular modeling were used to identify novel antagonists of liver receptor homolog-1 (LRH-1), an emerging therapeutic target for breast cancer. Hit compounds were synthesized and biologically assayed, and the preliminary results suggest that raloxifene-based analogues, substituted at the position C-7 of the benzothiophene ring, might generate an inactive protein conformation through binding and thus antagonize this nuclear receptor.



J. Rey, H. Hu, F. Kyle, C.-F. Lai, L. Buluwela, R. C. Coombes, E. A. Ortlund, S. Ali, J. P. Snyder,* A. G. M. Barrett**



Discovery of a New Class of Liver Receptor Homolog-1 (LRH-1) Antagonists: Virtual Screening, Synthesis and Biological Evaluation

